Motor planning modulates neural activity patterns in early human auditory cortex

Daniel J. Gale[1], Corson N. Areshenkoff [1,2], Claire Honda[2], Ingrid S. Johnsrude[5,6,7], J. Randall Flanagan[1,2], & Jason P. Gallivan*[1,2,3]

[1]Centre for Neuroscience Studies, [2]Department of Psychology, and [3]Department of Biomedical and Molecular Sciences, Queen's University, Kingston, Ontario, Canada. [5]Department of Psychology, School of Communication Sciences and Disorders[6], and [7]Brain and Mind Institute, University of Western Ontario

Abbreviated Title: Movement planning modulates auditory cortex

Number of Pages: 39

Number of words in Abstract: 168

Number of Figures: 4

Number of Supplemental Figures: 4

*Correspondence should be addressed to:

Jason Gallivan

Centre for Neuroscience Studies

Queen's University

gallivan@queensu.ca

Abstract

It is well established that movement planning involves the activation of motor-related cortical brain areas in preparation for the forthcoming action. Given that an integral component of the control of action is the processing of sensory information throughout movement, we predicted that movement planning also involves preparing early sensory cortical areas for participation in the impending behaviour. To test this hypothesis, we focused on activity in early human auditory cortex during the planning of an object manipulation task, known to involve predicting and evaluating discrete sensory events, including auditory events. We show, using functional MRI and a delayed object lifting task, that information related to the limb to be used to grasp and lift an object can be decoded, well before movement, from neural activity patterns in early auditory cortex. This suggests that action planning, in addition to preparing the motor system for movement, involves the task-specific preparation of primary sensory areas, such that they are set up to appropriately process sensory information arising during the unfolding movement.

Keywords

Motor, Planning, Audition, Auditory, Object manipulation, Action

Significance Statement:

The mammalian auditory system is characterized by an extensive, highly interconnected web of feedback projections, an architecture that, in humans, has been primarily implicated in sustaining auditory attention and facilitating working memory. Yet, its role in supporting the planning and control of everyday object-directed movements remains underappreciated and largely unstudied. Here we show, using neural decoding methods and a naturalistic object manipulation task, that hand movement planning modulates early auditory cortical activity patterns in an automatic, motor-specific fashion. These findings suggest that, prior to movement, the motor system prepares the neural state of early auditory cortex, readying it for the processing of sensory information during movement execution.

INTRODUCTION

Most theories of motor control distinguish between the planning of a movement and its subsequent execution. Research examining the neural basis of movement planning has commonly used delayed movement tasks—in which instructions about what movement to perform are separated in time from the instruction to initiate that movement—and has focused on delay period activity in motor-related brain areas. The conventional view has been that planning activity reflects the coding of one or more parameters—e.g., direction, extent, speed, curvature, force—of the forthcoming movement to be executed [1–8]. However, recent theories, which view neural activity from a dynamical systems perspective [9], offer a different interpretation; namely that movement planning involves preparing the initial neural state of the motor system, from which point movement execution evolves naturally through intrinsic neural processes [9–15]. To date, the focus of this work has been on understanding how changes in these neural activity patterns ultimately shape muscle activity [9,11,16].

A critical component of skilled action is the prediction of the sensory consequences of motor commands [17,18]. For example, the sensorimotor control of object manipulation tasks involves predicting the sensory signals associated with contact events, which define subgoals of the task [19,20]. Thus, when reaching towards, lifting, and then replacing an object, the brain predicts sensory signals linked to contact between the digits and the object, the breaking of contact between the object and the surface, and contact between the object and surface, respectively. Importantly, these signals can occur in multiple sensory modalities, including tactile, proprioceptive, visual, and auditory[19]. By comparing the predicted to actual sensory outcomes, the brain can monitor task progression, detect performance errors, and quickly launch appropriate, task-protective corrective actions as needed. Such compensatory behaviour will occur during task performance in cases where the anticipated auditory events fail to occur at the predicted time[21]. Sensory prediction is also critical in sensory cancellation, the attenuation of predictable sensory events that arise as a consequence of movement. Such attenuation

is thought to allow the brain to disambiguate sensory events that arise from movement from events that arise from external sources [22,23]. Given the functional importance of predicting task-specific sensory consequences, we hypothesize that action planning, in addition to preparing motor areas for execution, involves the preparation of primary sensory areas for processing task-specific sensory signals. Given that these sensory signals will depend on the precise action being performed, this hypothesis predicts that neural activity in early sensory areas will represent motor-related information prior to movement, during action planning.

As a critical test of this hypothesis, here we examined, using human functional MRI and a delayed object lifting task, whether the hand (left or right) used to lift the object can be decoded from delay period activity in early auditory cortex. We manipulated the hand used for lifting because the preparatory neural activity associated with left and right hand movements are very different at the level of the motor system [24,25]. We focused our analysis on early auditory cortex because of the role of auditory signals in the sensorimotor control of object manipulation tasks [19], and because of its known ipsilateral connections with the motor system in mammals [26,27]. Finally, although previous work has shown that auditory cortex is modulated by motor inputs during movement execution [28–33], the focus has been on real-time sensory attenuation, during movement execution, of the predictable sensory consequences of action. Here we instead focus on planning-related activity, and the broader function of motor signals in preparing early sensory areas for participation in forthcoming sensorimotor control.

RESULTS

To test our hypothesis that the motor system modulates the neural state of early auditory cortex during planning, we had 16 participants perform a delayed object lifting task, thereby allowing us to separate motor planning-related modulations from the later motor execution and somatosensory-related modulations. In effect, this delayed movement task allowed us to ask whether the hand action being prepared—but not yet

executed—can be decoded from neural activity patterns in early auditory cortex. To examine this, in each trial we had participants first prepare, and then execute (after a jittered delay interval) either a left or right hand object lift-and-replace action, which were cued by two nonsense auditory commands ("Compty" or "Midwig"; see Fig 1). Importantly, halfway throughout each experimental run, participants were required to switch the auditory command-to-hand mapping (i.e., if "Compty" cued a left hand object lift-and-replace action in the first half of the experimental run, then "Compty" would cue a right hand object lift-and-replace action in the second half of the experimental run; see Fig 1B). Critically, this allowed us to examine early auditory cortex activity on trials in which the exact *same* auditory command (e.g., "Compty"), and thus same sensory input, was being used to plan two distinct hand actions (left hand vs. right hand movements). As such, any neural differences in auditory cortex prior to movement on these trials are likely to reflect top-down modulations related to motor, and not sensory, processing.

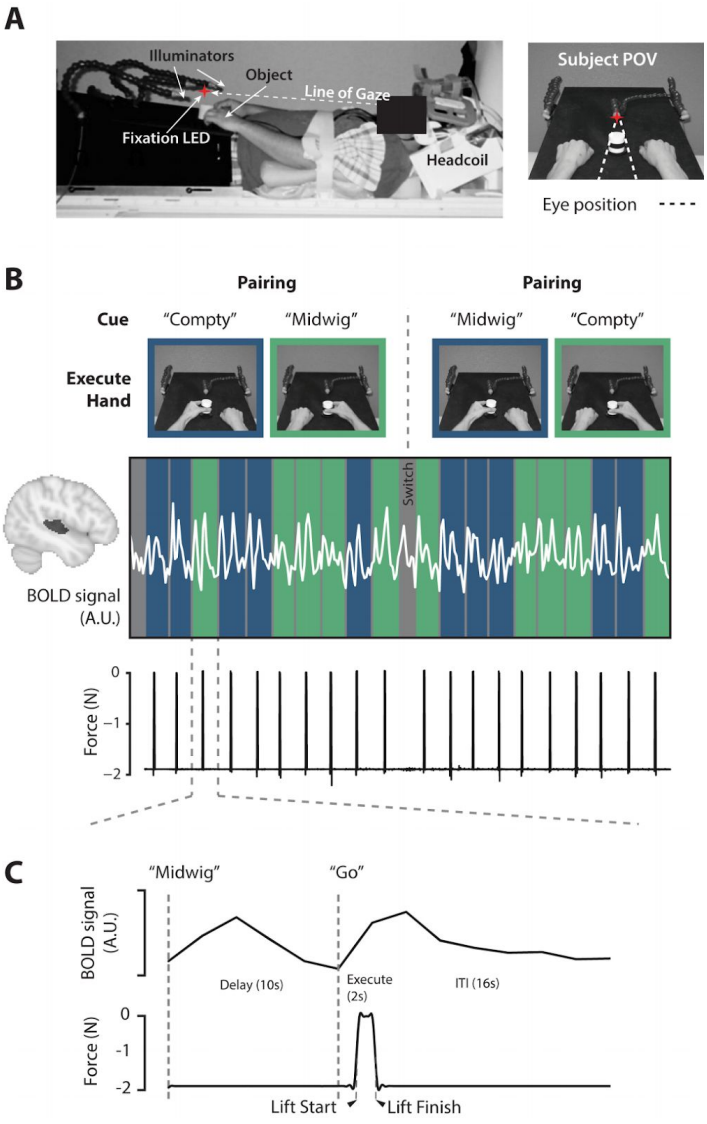

Figure 1. Experimental task and regions of interest
A. MRI setup (left) and subject point-of-view (right) of the experiment workspace. Red star indicates the fixation LED placed above the object. Illuminator LEDs, attached to the flexible stalks, are shown on the left and right. For anonymization purposes, a black box was placed over the subject's face. **B.** Example scanning run of 20 task trials. Color-coded columns (blue = left hand, green = right hand) demarks each trial and the associated time-locked BOLD activity from STG (shaded in dark gray on cortex, left) of an exemplar subject is indicated by the overlaid white trace. Pairings between auditory cue ("Compty" or "Midwig") and hand (left or right) are indicated above, and were reversed halfway through each run following a 'Switch' trial, such that each hand is paired with each auditory cue in every experimental run (see Methods). The corresponding force sensor data, used to track object lifting, is shown below. **C.** Sequence of events and corresponding single-trial BOLD and force sensor data of an exemplar trial from a representative participant in which 'Midwig' cued a right-handed movement. Each trial begins with the hand workspace being illuminated while, simultaneously, participants receive the auditory cue ("Compty" or "Midwig"). This is then followed by a jittered 6-12s Delay epoch (10s in the exemplar trial). Next, an auditory "Go" cue initiates the start of the 2s Execute epoch, during which the subject grasp-and-lifts the object (shown by the force trace; arrows indicate the start of the lift and object replacement). Following the Execute epoch, illumination of the workspace is extinguished and subjects then wait a fixed 16s intertrial interval (ITI) prior to onset of the next trial. See also Supplemental Fig. 1 for an overview of the trial sequence.

Delay period decoding of hand information from early auditory cortex

To determine whether signals related to hand movement planning influence early auditory cortex activity, we extracted the trial-related voxel patterns (beta coefficients) associated with the Delay and Execute epochs from early auditory cortex. To this end, we first functionally identified, using the data from an independent auditory localizer task, fMRI activity in the left and right superior temporal gyrus (STG). To provide greater specificity with regards to the localization of potential motor planning-related effects, we further delineated this STG cluster based on its intersections with Heschl's gyrus (HG) and the Planum Temporale (PT), two adjacent human brain regions associated with primary and higher-order cortical auditory processing, respectively (see Fig. 2A for our basic approach; [34]). Next, for each of these 3 regions (STG, and its subdivisions into HG and PT) we used their z-scored voxel activity patterns (removed of their mean signal), labelled according to hand (left hand vs. right hand), as inputs to an support vector machine (SVM) binary classifier. Our analysis (see Fig. 2B) on the resulting classification accuracies revealed that information related to the upcoming hand actions to be performed (i.e., during the Delay epoch) was present in all 3 left hemisphere auditory regions (STG, $t_{14} = 2.66$, $p = .009$; HG, $t_{14} = 2.70$, $p = .009$; PT, $t_{14} = 5.29$, $p < .001$), but absent in the right hemisphere (STG, $t_{14} = 1.44$, $p = .086$; HG, $t_{14} = 1.24$, $p = .118$; PT, $t_{14} = 1.07$, $p = .151$). During the Execute epoch, however, we found that hand-related decoding was robust in all three areas in both hemispheres (all $p < 10^{-5}$). Because our task did not pair the hand movements to sound generation, and subjects would not have heard the auditory consequences associated with movement (e.g., object lifting and replacement) due to the loud background noise of the scanner, these results suggest that the lateralized modulation of auditory cortex activity is automatic and motor-related in nature[27].

In contrast to our hand decoding results, our analysis on the resulting classification accuracies associated with a main effect of auditory cue ("Compty" vs. "Midwig") revealed that, during the Delay epoch, information related to the delivered verbal cue

was present in left and right STG (left, $t_{14} = 2.13$, $p = 0.026$; right, $t_{14} = 2.90$, $p = 0.006$), and left PT ($t_{14} = 3.86$, $p < .001$). No effects were found in the remaining ROIs (all $p > .10$). Consistent with the fact that this auditory cue information was presented only during the Delay epoch (i.e., participants always received a “Go” cue at the Execute epoch), we also observed no evidence of cue-related decoding during the Execute epoch (all $p > .10$). Taken together, this pattern of results suggests that, unlike auditory cue information, the representation of hand-related information during the Delay epoch is: (1) lateralized to the left hemisphere, and (2) present in both core (HG) and belt/parabelt (PT) auditory cortex. An additional behavioural control experiment, performed prior to MRI testing, suggests that the emergence of these hand-related effects are unlikely to be driven by systematic differences in eye position across trials [35], since our trained participants exhibited highly stable fixations throughout the task (see Supplemental Fig. 1).

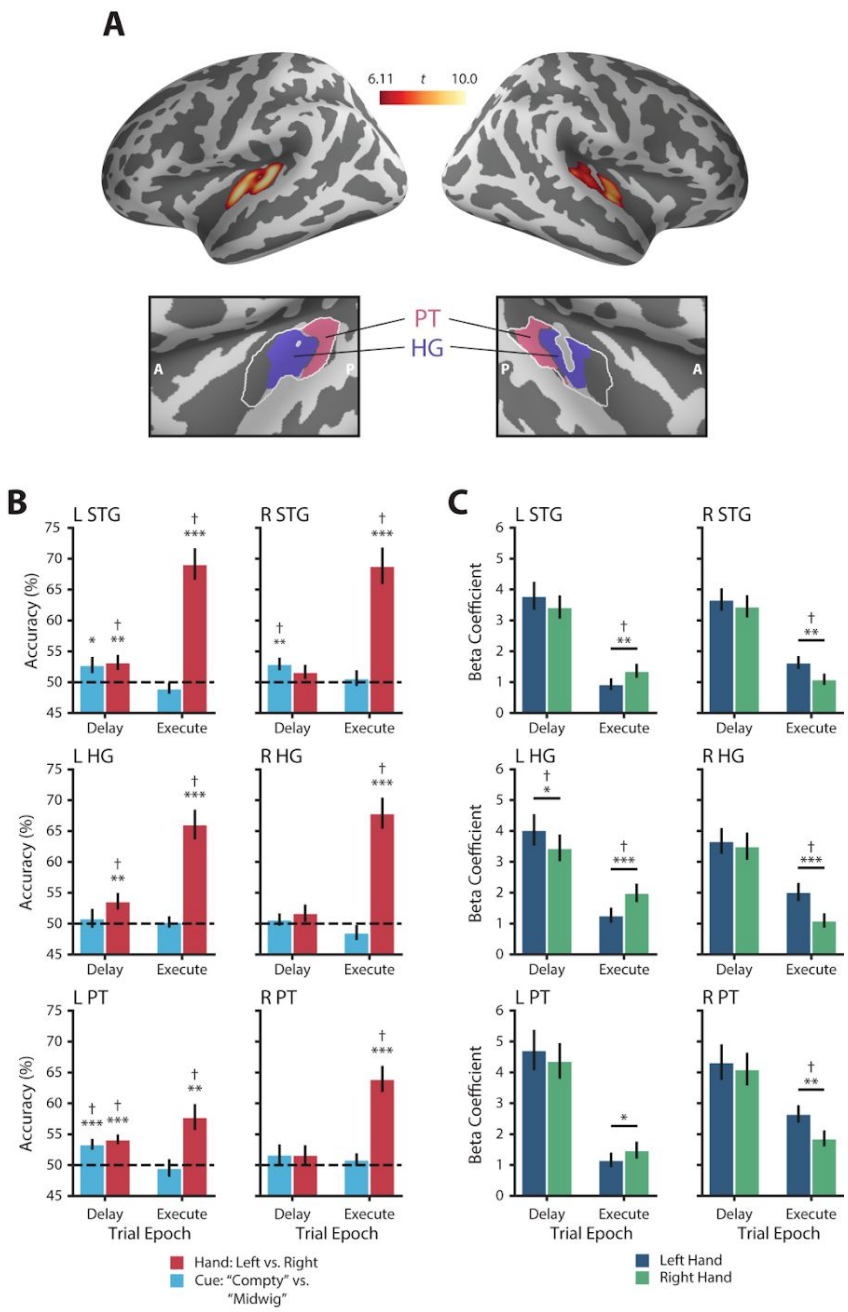

Figure 2. Multivariate, but not univariate analyses, reveal the coding of hand information during the Delay epoch activity in early auditory cortex. **A.** Top, left and right STG clusters defined at the group-level (N = 16) with the auditory localizer task using the contrast of Scrambled > Rest. Below, Heschl's gyrus (HG) and Planum Temporale (PT), delineated within each STG cluster (white trace). **B.** Decoding accuracies for hand (red) and cue (blue) information. Hand and cue decoding accuracies were analyzed separately in each epoch using one-sample t-tests (one-tailed) against chance level (50%). **C.** Mean beta coefficients derived from averaging trialwise betas for left hand and right hand trials. Magnitudes of left hand and right hand trials were compared using paired t-tests at each epoch. Error bars show ± 1 SE of mean. * p < .05, ** p < .01, *** p < .001, † FDR corrected q < .05.

Hand-related signals are present in multivariate, not univariate, information

Although the spatial voxel patterns used for pattern classification were z-scored, we still wondered whether hand-related information was also present within the mean univariate signal of each auditory cortex region. To examine this in our data, we computed, for each trial and epoch (Delay and Execute), the mean beta coefficient

value across the voxel pattern and then compared these across participants for left hand and right hand trials using paired t-tests (see Fig. 2B). During the Delay epoch, beta coefficients did not significantly differ between the left hand and right hand in any region, except left HG (t_{14} = 2.35, p = .034). However, during the Execute epoch, we found that contralateral hand information was represented quite robustly in the mean univariate signal. For instance, in left STG and HG, right hand trials evoked greater activity than left hand trials (left STG, t_{14} = 3.21, p = .006; left HG, t_{14} = 4.30, p < .001); this effect was also shown in left PT (t_{14} = 2.33, p = .035), but it did not survive FDR-correction (q = .071). By contrast, right auditory regions showed the opposite effect wherein activity on left hand trials was greater than on right hand trials (right STG, t_{14} = 3.58, p = .003; right HG, t_{14} = 4.97, p < .001; right PT, t_{14} = 3.99, p = .001). Thus, unlike movement planning and consistent with recent reports [36], movement execution elicits selectively enhanced univariate activity in the auditory cortex contralateral to the hand being used. [For interested readers, we also report, in Supplemental Fig. 2, an univariate analysis related to the auditory cue, i.e., “Compty” vs. “Midwig”]. Taken together, these results show that hand-related information during planning can be revealed in auditory cortex largely in the absence of univariate effects.

Time-resolved decoding reveals that hand information in auditory cortex emerges just prior to movement onset

One possible alternative interpretation of our above finding showing the decoding of hand information during the Delay epoch is that, rather than it reflecting a top-down, motor-related modulation, it instead reflects the fact that participants, in our task, must map the auditory command onto a hand instruction. Specifically, upon receiving an auditory cue (e.g., “Compty”), it is plausible that participants immediately translate that cue into the actual instructed action (i.e., think to themselves that “Compty” means “Left Hand”). If so, then it could be the case that it is this auditory conversion or sensory transformation process that is being decoded in auditory cortex, and being interpreted here as the representation of motor effector-specific signals. If this were true, we would then predict that the decoding of hand information should occur at very similar points in

time during the trial than the decoding of cue information (i.e., under the assumption that participants would directly transform the nonsense auditory cue “Compty” into the auditory cue “Left Hand”, for example). By contrast, if the decoding of hand information is linked to top-down influence from the motor system, then we would instead predict that the emergence of hand-related information should occur immediately prior to, and at, movement onset (i.e., the decoding of cue and effector information should be decoupled in time). However, because our above pattern decoding analyses were based on beta coefficient measures (reflecting the correspondence between the Delay epoch BOLD time-course signal and a convolved HRF), this approach lacks the necessary time resolution to disentangle these different interpretations. Thus, to directly test this potential alternative explanation of our results, we performed single time-point decoding throughout the trial in our main STG clusters, thereby allowing us to assess not only if, but also when, cue and hand information arises during the Delay epoch (for similar approaches see [37–39]).

This single-time point decoding approach in the STG revealed that, whereas cue information (“Compty” vs. “Midwig”) was commonly decoded within the third imaging volume during the Delay epoch (i.e., the 4-6 s time window, approximately corresponding to the peak % BOLD response in the time course signal), hand information was instead decoded in the final imaging volume of the Delay epoch and/or immediately at the onset of the “Go” cue (see Fig. 3). This was despite the fact that the % BOLD time course signal in STG at those time points was at near-baseline levels. This timing of hand-related decoding is noteworthy considering that the earliest latencies we expect to reliably observe an event-induced BOLD effect are at least 2 seconds following that event [40]; thus, this means that decoding at the final imaging volume of the Delay epoch likely reflects neural events preceding it by at least 2 seconds. As such, it is unlikely that our hand-related decoding effects during the Delay epoch solely reflect a sensory attenuation effect, as these have been shown to occur in auditory cortical neurons ~200 ms prior to movement onset [27]. Following the onset of the

“Go” cue, we found that decoding accuracies subsequently rose during the Execute epoch, with the time point associated with the peak decoding accuracy generally corresponding to the peak % BOLD response in the time course signal.

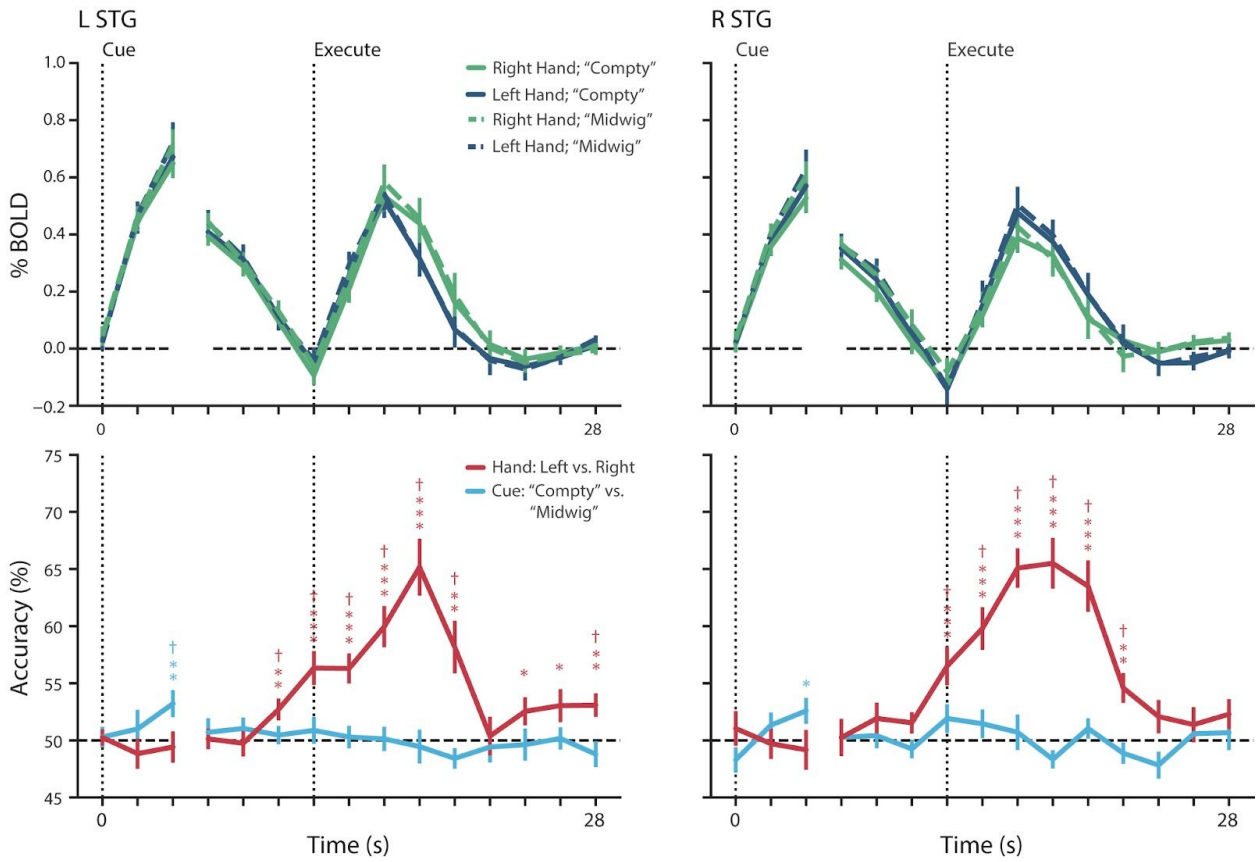

Figure 3. Time-resolved decoding analysis reveal that auditory cue and hand-related information are represented a different time points prior to movement onset. Top, group-averaged percent signal change values of each condition. Bottom, group-level decoding accuracies obtained by separately analyzing hand and auditory cue decoding at each timepoint. Each time point was tested against chance accuracy (50%, horizontal dashed line) using one-sample t-test (one-tailed). The first three time points are time-locked to the onset of the Delay epoch (in which subjects hear the auditory cue), and the remaining 12 time points are time-locked to the onset of the Execute epoch. Error bars show ± 1 SE of mean. Significance markers are colored according to factor (red, hand; blue, cue), * $p < .05$, ** $p < .01$, *** $p < .001$, † FDR corrected $q < .05$.

To provide a basis for comparing and interpreting these above effects, we also used the data from our Experimental task to examine time-resolved decoding in a positive control

region, the dorsal premotor cortex (PMd). This region is well known to be involved in limb-related movement planning in both humans and nonhuman primates [24,41] and was independently identified using our motor localizer data. As shown in Supplemental Fig. 3, we find a strikingly similar profile of limb-specific decoding in this motor-related region to that observed in STG. In fact, we found that a direct comparison between the magnitude of hand-related decoding in STG and PMd were non-significant at the time-point prior to, and during, the Execute epoch (see Supplemental Fig. 3E, bottom plot). Taken together, this single-time point decoding approach allows for two important observations. First, similar levels of action-related information can be decoded from early auditory cortex as from dorsal premotor cortex, the latter area known to have a well-established role in motor planning [42–44]. Second, these time-resolved decoding analyses indicate that the representation of cue and hand-related information are decoupled in time during the Delay epoch, lending support for the interpretation that hand-related decoding does not simply reflect some mental auditory rehearsal of the instructed action.

Searchlight analyses reveal the representation of hand information in early auditory cortex during planning

To complement our above ROI analyses, we also performed a group-level searchlight analysis within the wider auditory processing network, localized using our independent auditory localizer data (see Methods, Supplemental Fig. 4A). We found that hand-related decoding during the Delay epoch was constrained to a single cluster in left auditory cortex (229 voxels; peak, x = -50, y = -22, z = 8, $t_{14} = 6.06$, $p < .001$), replicating our basic pattern of ROI-based results (see Fig. 4A,B). [We also report the uncorrected searchlight results in Supplemental Fig. 4B, which highlights several regions (e.g., cerebellum, anterior temporal pole, right STG) that did not pass cluster correction].

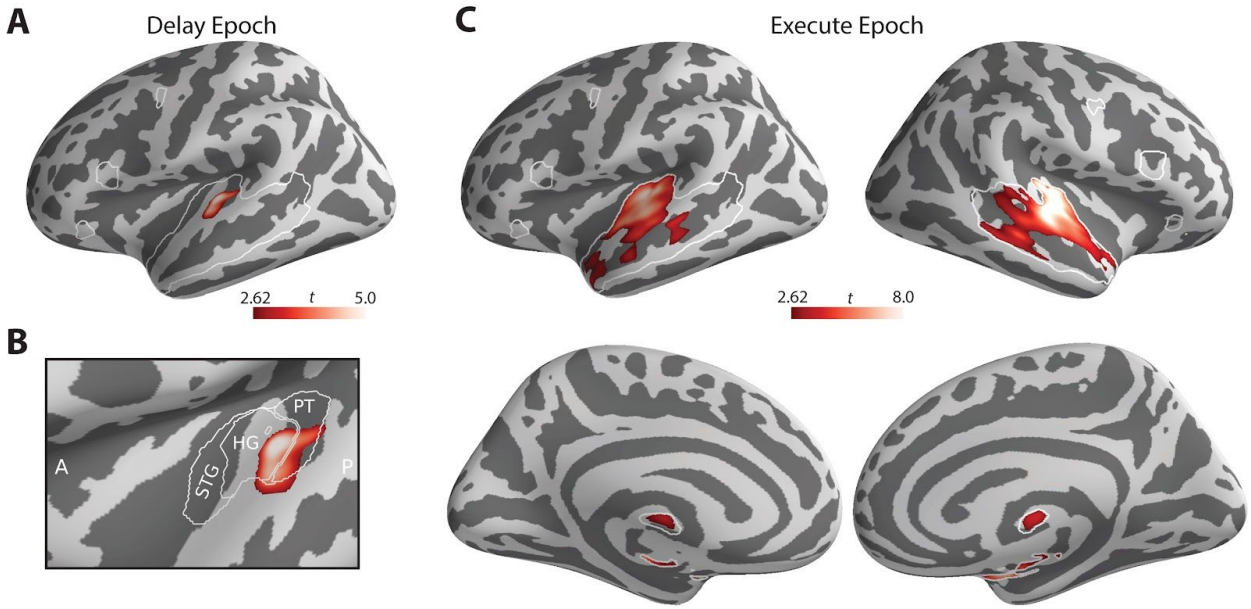

Figure 4. Searchlight analyses within a higher-order auditory network reveal that the representation hand information during the Delay epoch is constrained to early auditory cortex. Searchlight analyses were restricted to a mask defined by significant voxels in a Intact > Scrambled contrast using the auditory localizer task (white trace; see Methods). Group-level searchlight maps were thresholded at $t > 2.62$ (one-tailed $p < .01$) and cluster-corrected at $p < .05$. **A.** Map of hand-related decoding during the Delay epoch, which reveals a single cluster in left STG. **B.** Overlay of the Delay epoch decoding cluster with traces corresponding to the left auditory regions analyzed in ROI analyses. **C.** Lateral and medial views of the left and right hemispheres for hand-related decoding during the Execute epoch.

A searchlight analysis using the Execute epoch data revealed a far more extensive pattern of hand-related decoding throughout the auditory network, with significant trial classification extending all along the superior and middle temporal gyri bilaterally, and even into the basal ganglia and medial temporal cortex, medially (see Fig. 4C). This far more diverse pattern of effects is to be expected given the natural auditory, visual, tactile and proprioceptive consequences associated with actual movement generation. These searchlight findings, when considered jointly with our ROI-based results, provide strong supporting evidence that movement planning selectively modulates neural activity patterns in early auditory cortex.

DISCUSSION

We have shown, using fMRI and a delayed object lifting task, that the hand used for lifting can be decoded from pre-movement (i.e., delay period) neural activity patterns in early auditory cortex. Importantly, this decoding was independent of the auditory cue used to instruct the participant on which hand to use, and occurred at a later time point than the decoding of this cue. These findings suggest that a critical component of action planning, beyond preparing motor areas for the forthcoming movement, is preparing early sensory areas. Such preparation may enable these areas to more effectively participate in filtering and processing task-specific sensory signals that arise during the unfolding movement itself.

Several hypotheses have been proposed about the role of planning-related activity in motor areas, including the primary, premotor, and supplementary motor cortices. Several researchers have suggested that planning activity encodes a variety of different movement parameters (e.g., direction), with a view that it represents some subthreshold version of the forthcoming movement [1–8]. Recent work, examining the dynamics of populations of neurons in motor areas, has instead suggested that movement planning involves setting up the initial state of the population, such that movement execution can unfold naturally through transitory neural dynamics [9,11,12,15,43,45]. Within this framework, our results suggest that motor planning may also involve preparing the initial state of primary sensory cortical areas. Whereas the neural activity patterns that unfold during movement execution in motor areas are thought to regulate the timing and nature of descending motor commands [9,11],such activity in primary sensory areas may instead regulate the timing and nature of the filtering of incoming sensory signals.

Motor planning signals could, in principle, tune early sensory areas for participation in sensory prediction. Prediction of the sensory consequences of movement is essential for the accurate sensorimotor control of movement, per se, and also provides a

mechanism for distinguishing between self-generated and externally generated sensory information [46]. The critical role of prediction in sensorimotor control has been well documented in the context of object manipulation tasks [20,47]. The control of such tasks centers around contact events, which give rise to discrete sensory signals in multiple modalities (e.g., auditory, tactile) and represent subgoals of the overall task. Thus, in the grasp, lift, and replace task that our participants performed, the brain predicts the timing and nature of discrete sensory signals associated with contact between the digits and object, as well as the breaking, and subsequent making, of contact between the object and surface; events that signify successful object grasp, lift-off, and replacement, respectively. By comparing predicted and actual sensory signals associated with these events, the brain can monitor task progression and launch rapid corrective actions if mismatches occur [17]. These corrective actions are themselves quite sophisticated and depend on both the phase of the task and the nature of the mismatch [48]. Thus, the planning of manipulation tasks clearly involves forming what could be referred to as a 'sensory plan'; i.e., a series of sensory events—linked to contact events—that, during subsequent movement execution, can be predicted based on knowledge of object properties and information related to outgoing motor commands [46,47].

The disambiguation of self- and externally generated sensory information is thought to rely on cancelling, or attenuating, the predictable sensory consequences of movements [46]. Such 'sensory cancellation' has been investigated in the context of tasks involving manual interactions with objects. It has been shown, for example, that when participants use one index finger to tap a disk mounted above the other index finger, the perceived force—acting on the lower finger—is attenuated relative to when the same tap is delivered by an electric motor [49]. Importantly, this attenuation is not linked to movement, *per se*, but is temporally tuned to the timing of the predicted contact event [50,51].

Sensory predictions for use in *sensory cancellation* are generally thought to be represented in primary sensory areas. According to this view, an efference copy of

descending motor commands, associated with movement execution, is transmitted in a top-down fashion to early sensory cortices in order to attenuate self-generated sensory information [23,52]. In contrast, sensory predictions, for use in *sensorimotor control*, are thought to be represented in the same frontoparietal circuits involved in movement planning and control [53,54]. According to this view, incoming sensory information, associated with movement execution, is transmitted in a bottom-up fashion from early sensory areas to frontoparietal circuits for mismatch detection and movement correction [55–57]. However, our understanding of sensory prediction in the context of sensorimotor control remains quite limited, and whether it involves the top-down modulation of sensory areas has remained an open question.

Critically, the modulation of early auditory cortex we observed occurred well in advance of movement execution, and is thus unlikely to solely reflect sensory cancellation or on-line sensorimotor control. Indeed, sensory attenuation responses in primary auditory cortex have been shown to occur about two hundred milliseconds prior to movement onset (Schneider 2014; 2018), whereas the hand-specific modulation of auditory cortex we report occurred several *seconds* prior to movement onset. Notably, we showed that this modulation occurred at similar points in time, prior to movement, as the emergence of hand-related decoding in premotor cortex (see supplemental data). Thus, one possible explanation for the pre-movement modulation of auditory cortex is that it arises from the motor system preparing the state of auditory cortex to process auditory inputs in a task- and phase-dependent manner. Support for this notion comes from the fact that, in the scanner environment, our participants could not have heard the auditory consequences of their actions; e.g., sounds associated with contacting, lifting, and replacing the object. This argues that our reported pre-movement modulation of auditory cortex has a motor-related origin, and is not linked to sensory reafference or attentional processes [58,59]. Moreover, it suggests that this modulation arises from automatic processes that occur during movement planning.

Prior work has also demonstrated that tactile input alone is capable of driving auditory cortex activity [60–63], indicating a potential role for auditory cortex in multisensory integration. As noted above, the control of object manipulation tasks involves accurately predicting discrete sensory events that arise in multiple modalities, including tactile and auditory [64]. It is plausible then that some portion of the pre-movement auditory cortex modulation described here reflects the predicted tactile events arising associated from our task (e.g., object contact, lift-off and replacement), which we would also expect to be linked to the acting hand. Though we cannot disentangle this possibility in the current study, it is a direction for future work and does not undercut our main observation that early sensory cortex is modulated as a function of the movement being prepared, nor its interpretation, that such modulation is likely linked to sensory prediction.

When considering the topological organization of sensory and motor systems, we find it noteworthy that, during the delay period, the decoding of hand-related information was lateralized to left auditory cortex. At first glance, such lateralization appears at odds with the known bihemispheric connections between ipsilateral motor and auditory areas in both rodents [30,65–67] and nonhuman primates [68–71]. In humans, however, there exist well-documented left hemispheric specializations for both auditory [72,73] and sensorimotor-related processing [74–76], particularly in right-handed individuals (as our participants were). Specifically, two major fiber tracts in humans, the arcuate and the uncinate fasciculi, are thought to support significant auditory-motor interactions during vocalization and sound-producing behaviours [77]. This lateralization of network architecture provides a likely neuroanatomical basis for our observations.

In summary, here we show that, prior to movement, neural activity patterns in early auditory cortex carry information about the hand to be used in the upcoming action. This result supports the hypothesis that ‘motor’ planning, which is critical in preparing neural states ahead of movement execution [43], not only occurs in motor areas but also in

primary sensory areas. Further work is required to establish the precise role of this movement-related modulation. Our findings add to a growing line of evidence indicating that early sensory systems are directly modulated by sensorimotor computations performed in higher-order cortex [78–81] and not merely low-level relayers of incoming sensory information [82–85].

METHODS

Participants

Sixteen healthy right-handed subjects (8 females, 21-25 years of age) participated in one behavioural testing session followed by two fMRI testing sessions (a localizer testing session, and the Experimental testing session, performed on separate days approximately 1-2 weeks apart). Right-handedness was assessed with the Edinburgh handedness questionnaire [86]. Informed consent and consent to publish were obtained in accordance with ethical standards set out by the Declaration of Helsinki (1964) and with procedures cleared by the Queen's University Health Sciences Research Ethics Board. Subjects were naïve with respect to the hypotheses under evaluation and received monetary compensation for their involvement in the study. Data from one subject were excluded from further analyses in our Experiment due to problems in data collection, resulting in a final sample size of 15 subjects.

Experimental apparatus

The experimental setup for both the localizer and experimental testing sessions consisted of a black platform placed over the waist and tilted away from the horizontal at an angle (~15°) to maximize comfort and target visibility. The MRI head coil was tilted slightly (~20°) and foam cushions were used to give an approximate overall head tilt of 30°. To minimize limb-related artifacts, subjects had the right and left upper-arms braced, limiting movement of the arms to the elbow and thus creating an arc of reachability for each hand. The exact placement of object stimuli on the platform was adjusted to match each subject's arm length such that all required actions were comfortable and ensured that only movement of the forearm, wrist and fingers was required (when relevant). The platform was illuminated by two bright white Light Emitting Diodes (LEDs) attached to flexible plastic stalks (Loc-Line, Lockwood Products, Lake Oswego, OR, USA) located to the left and right of the platform. To control for eye movements, a small red fixation LED, attached to a flexible plastic stalk, was positioned

above the hand workspace and located ~5 cm beyond the target object positions (such that they appeared in the subject's lower visual field). Experimental timing and lighting were controlled with in-house software created with C++ and MATLAB (The Mathworks, Natnick, MA). Throughout the fMRI studies, the subject's hand movements were monitored using an MR-compatible infrared-sensitive camera (MRC Systems GmbH, Heidelberg, Germany), optimally positioned on one side of the platform and facing towards the subject. The videos captured during the experiment were analyzed offline to verify that the subjects were performing the task as instructed and identify error trials.

Motor Localizer task

In short, the motor localizer task constituted a block-design protocol, which alternated between subtasks designed to localize eight separate motor functions. The hand grasping condition in this study was used to localize the activity in dorsal premotor cortex (PMd), used for comparison with early auditory cortex decoding. For details on this localizer task, please see the *Supplemental Material*.

Auditory Localizer Task

A separate, block-design localizer task was collected alongside the Motor Localizer task to independently identify auditory cortex and higher-order language regions of interest (ROIs) for use in the analyses of Experimental task. This Auditory Localizer task included three conditions: (1) Intact speech trials (Intact), which played one of 8 unique excerpts of different speeches; (2) scrambled speech trials (Scrambled), which were incoherent signal-correlated noise versions of the speech excerpts (i.e. applying an amplitude envelope of the speech to uniform Gaussian white noise, ensuring that the noise level was utterance-specific and exactly intense enough at every moment to mask the energy of the spoken words); and (3) rest trials (Rest), in which no audio was played (subjects thus only heard background MRI scanner noise). Trials lasted 20 s each and alternated, in pseudo-random order, between Intact, Scrambled, and Rest for a total of 24 trials in each experimental run. In addition, a 20 s baseline block was placed at the

beginning of each experimental run. Each localizer run totaled 500 s and participants completed 2 of these runs during testing (resulting in 16 repetitions per experimental condition per subject). To encourage that participants maintain attention throughout this auditory localizer run, they were required to monitor each of the Intact speeches and let the experimenter know, following the run, whether any of them were repeated. This repeat happened in only one of the experimental runs and every subject correctly identified the repeat and non-repeat run (100% accuracy).

The motor and auditory localizer testing session lasted approximately 2 hours and included set-up time, one 7.5 minute high-resolution anatomical scan and 6 functional scanning runs, wherein subjects alternated between performing two runs of the motor localizer task and one run of the auditory localizer, twice. A brief (~10 minute) practice session was carried out before the localizer testing session in the MRI control room in order to familiarize participants with localizer tasks.

Experimental Task

In our experimental task (see Fig. 1), we used a delayed movement paradigm wherein, on each individual trial, subjects were first auditorily cued (via headphones) to prepare either a left (left hand) vs. right hand (right hand) object grasp-and-lift action on a centrally located cylindrical object (1.9 N weight). Then, following a variable delay period, they were prompted to execute the prepared hand action. At the start of each event-related trial (see Fig. 1C), simultaneously with the LED illuminator lights going on (and the subject's workspace being illuminated), subjects received one of two nonsense speech cues, "Compty" or "Midwig". For a given trial, each nonsense speech cue was paired with a corresponding hand action (e.g., subjects were instructed that, for a predetermined set of trials, "Compty" cued a left hand movement whereas "Midwig" cued a right hand movement). [Note that nonsense speech commands were chosen because semantically meaningful words such as "left" and "right" would already have strong cognitive associations for participants.] Following the delivery of the auditory

command, there was a jittered delay interval of 6-12 s (a Gaussian random jitter with a mean of 9 s), after which the verbal auditory command “Go” was delivered, prompting subjects to execute the prepared grasp-and-lift action. For the execution phase of the trial, subjects were required to precision grasp-and-then-lift the object with their thumb and index finger (~2 cm above the platform, via a rotation of the wrist), hold it in midair for ~1 s, and then replace it. Subjects were instructed to keep the timing of each hand action as similar as possible. Two seconds following the onset of this “Go” cue, the illuminator lights were extinguished, and subjects then waited 16 s for the next trial to begin (intertrial interval, ITI). Throughout the entire time course of the trial, subjects were required to maintain gaze on the fixation LED.

These event-related trials were completed in two separate blocks per experimental run. At the beginning of each experimental run, the experimenter informed subjects of the auditory-motor mapping to be used for the first 10 event-related trials of the experimental run (e.g. “Compty” for left hand (left hand) movements, “Midwig” for right hand (right hand) movements; 5 trials of each type). After the 10th trial, the illuminator was turned on (for a duration of 6 s) and subjects simultaneously heard the auditory command “Switch” (following by a 16 s delay), indicating that the auditory-motor mapping would now be reversed for the remaining 10 event-related trials (i.e., “Compty” would now cue a right hand movement whereas “Midwig” would now cue a left hand movement). The sequential ordering of this auditory-motor mapping was counterbalanced across runs, and resulted in a total of 4 different auditory-motor mappings (and thus, trial types) per experimental run: Compty-left hand, Compty-right hand, Midwig-left hand, and Midwig-right hand (with 5 repetitions each; 20 trials in total per run). With the exception of the blocked nature of these trials, these trial types were pseudorandomized within a run and counterbalanced across all runs so that each trial type was preceded and followed equally often by every other trial type across the entire experiment.

Separate practice sessions were carried out before the actual fMRI experiment to familiarize subjects with the delayed timing of the task. One of these sessions was conducted before subjects entered the scanner (See *Behavioural Control Experiment* below) and another was conducted during the anatomical scan (collected at the beginning of the Experimental task testing session). The Experimental task testing session for each subject lasted approximately 2 hours and included set-up time, one 7.5 minute high-resolution anatomical scan (during which subjects could practice the task) and eight functional scanning runs (for a total of 160 trials; 40 trials for each auditory-motor mapping). Each functional run (an example run shown in Fig. 1B) had a duration of 576 s, with a 30-60 s break in between each run. Lastly, a resting state functional scan, in which subjects lay still (with no task) and only maintained gaze on the fixation LED, was performed for 12 minutes (*data not analyzed here*).

During MRI testing, we also tracked subjects behaviour using an MRI-compatible force sensor located beneath the object (Nano 17 F/T sensors; ATI Industrial Automation, Garner, NC), and attached to our MRI platform. This force sensor, which was capped with a flat circular disk (diameter of 7.5 cm), supported the object. The force sensor measured the vertical forces exerted by the object (signals sampled at 500 Hz and low-pass filtered using a 5th order, zero-phase lag Butterworth filter with a cutoff frequency of 5 Hz), allowing us to track both subject reaction time (RT), which we define as the time from the “Go” cue to object contact (Mean = 1601ms, SD = 389ms), and movement time (MT), which we define as the time from object lift to replacement (Mean = 2582ms, SD = 662ms), as well as generally monitor task performance. Note that we did not conduct eye tracking during this or any of the other MRI scan sessions because of the difficulties in monitoring gaze in the head-tilted configuration with standard MRI-compatible eye trackers (due to occlusion from the eyelids)[78,87,88].

Data Acquisition and Analysis

Subjects were scanned using a 3-Tesla Siemens TIM MAGNETOM Trio MRI scanner located at the Centre for Neuroscience Studies, Queen's University (Kingston, Ontario, Canada). Functional MRI volumes were acquired using a T2*-weighted single-shot gradient-echo echo-planar imaging acquisition sequence (time to repetition = 2000 ms, slice thickness = 4 mm, in-plane resolution = 3 mm x 3 mm, time to echo = 30 ms, field of view = 240 mm x 240 mm, matrix size = 80 x 80, flip angle = 90°, and acceleration factor (integrated parallel acquisition technologies, iPAT) = 2 with generalized auto-calibrating partially parallel acquisitions reconstruction). Each volume comprised 35 contiguous (no gap) oblique slices acquired at a ~30° caudal tilt with respect to the plane of the anterior and posterior commissure (AC-PC), providing whole-brain coverage. Subjects were scanned in a head-tilted configuration, allowing direct viewing of the hand workspace. We used a combination of imaging coils to achieve a good signal to noise ratio and to enable direct object workspace viewing without mirrors or occlusion. Specifically, we tilted (~20° degrees) the posterior half of the 12-channel receive-only head coil (6-channels) and suspended a 4-channel receive-only flex coil over the anterior-superior part of the head. A T1-weighted ADNI MPRAGE anatomical scan was also collected (time to repetition = 1760 ms, time to echo = 2.98 ms, field of view = 192 mm x 240 mm x 256 mm, matrix size = 192 x 240 x 256, flip angle = 9°, 1 mm isotropic voxels).

fMRI data preprocessing

The fMRI preprocessing workflow consisted of routines from the FMRIB Software Library toolbox 5.0 (FSL, http://www.fmrib.ox.ac.uk, see [89]) and Statistical Parametric Mapping (SPM12; [90], which were implemented in Python 3.7.1 with Nipype v0.13.1 [91].

Each subject's anatomical scan first underwent brain extraction (FSL brain extraction tool) in order to remove non-brain tissue (e.g. skull), followed by nonlinear warping to

the standard MNI152 brain template (voxel size = 2 × 2 × 2 mm; FSL FNIRT). Functional scans were motion aligned to the volume closest to the anatomical scan using a six parameter affine transformation, and slice-time corrected for interleaved slice acquisition via Fourier-space time-series phase shifting (FSL slicetime). Spatial normalization of functional scans to the standard MNI152 template involved applying the 12 degrees-of-freedom linear affine transformation matrix obtained from coregistration to the anatomical scan (FSL FLIRT) combined with the warp field obtained from the nonlinear warping of the anatomical scan. Normalized functional scans were then temporally filtered using a high-pass filter (cutoff = 0.01 Hz) to remove low-frequency noise (e.g. linear scanner drift), and, in the case of the localizer tasks, were spatially smoothed (6mm FWHM Gaussian kernel; SPM12) prior to GLM estimation to facilitate subject overlap. [Note that no spatial smoothing was performed on the Experimental task data set, wherein multi-voxel pattern analyses were performed.]

These preprocessing steps ensured that scans were as unaffected by motion and scanner-related artifacts as possible, and that they could be analyzed in a common anatomical space. In addition, functional data from each testing session in each participant were screened for motion and/or magnet artifacts by examining the time-course movies and the motion plots created with the motion correction algorithms. None of the runs revealed head motion that exceeded 1.5 mm translation or 1.5° rotation. Error trials were identified offline from the videos recorded during the experimental testing session and were excluded from analysis by assigning these trials predictors of no interest. Error trials included those in which the subject performed the incorrect instruction (9 trials, 4 subjects) or contaminated the delay phase data by slightly moving their limb or moving too early (7 trials, 4 subjects). That subjects made so few errors considering the potentially challenging nature of the task (e.g., having to remember whether “Compty” cued a left hand or right hand movement on the current trial) speaks to the fact that subjects were fully engaged during experimental testing and very well practiced at the task prior to participating in the experiment.

Statistical Analyses

General Linear Models

For the localizer task analyses, we carried out subject-level analysis using SPM12's first-level analysis toolbox to create general linear models (GLM) for each task (auditory and motor). Each GLM featured condition predictors created from boxcar functions convolved with a double-gamma hemodynamic response function (HRF). These were aligned to the onset of each action/stimulus block, with its duration dependent on block length (i.e., 10 imaging volumes for both localizer tasks). Temporal derivatives of each predictor and subjects' six motion parameters obtained from motion correction were added as regressors to improve model fit. The Baseline/Fixation epochs were excluded from the model; therefore all regression coefficients (betas) were defined relative to the baseline activity during these time points.

In the Experimental task, separate GLM models for each individual trial's Delay and Execute epochs were generated in order to extract beta coefficient estimates for decoding analyses (20 trials x 2 epochs x 8 runs = 320 GLMs). The regressor of interest in each model consisted of a boxcar regressor aligned to the start of the epoch, with an impulse duration (0 s) set for the Delay epoch and a duration of 2s for the Execute epoch. We included a second regressor that was comprised of all remaining trial epochs in the experimental run. Each regressor was then convolved with a double-gamma HRF, and temporal derivatives of both regressors were included along with subjects' six motion parameters obtained from motion correction. Isolating the regressor of interest in this single-trial fashion reduces regressor collinearity, and has been shown to be advantageous in estimating single trial voxel patterns and for multi-voxel pattern classification [92].

Region of interest (ROI) selection

Regions of interests (ROI) were identified based on second-level (group) analyses of first-level contrast images from each subject. Early auditory cortex ROIs were identified by thresholding a Scrambled > Rest group contrast at an uncorrected voxelwise threshold of $p < 10^{-5}$. This procedure identified tight superior temporal gyrus (STG) activation clusters in left and right Heschl's gyrus (HG), the anatomical landmark for primary (core) auditory cortex [93–96], and more posteriorly on the superior temporal plane (Planum Temporale, PT). We verified these locations by intersecting region masks for HG and PT obtained from the Harvard-Oxford anatomical atlas[97] with the masks of left and right STG clusters. This allowed us to define, for each participant, voxels that were active for sound that fell in anatomically defined HG and PT. We considered HG and PT separately since they are at different stages of auditory processing: HG is the location of the core, whereas the PT consists of belt and probably parabelt regions, as well as possibly other types of cortical tissue [98]. Since our PT activity is just posterior to HG, we suspect that this is probably in belt or parabelt cortex, one or two stages of processing removed from core. Lastly, a wider network involved in higher-order auditory and speech processing was obtained using a cluster Intact > Scrambled contrast with an uncorrected height threshold of $p < .001$ and cluster-extent correction threshold of $p < .05$. Together, these were used as three-dimensional binary masks to constrain our analyses and interpretations of motor-related effects to the auditory system.

Multi-voxel Pattern Analysis (MVPA)

For the Experimental task, MVPA was performed with in-house software using Python 3.7.1 with Nilearn v0.5.0 and Scikit-Learn v0.20.1 [99]. All analyses implement linear support vector machine (SVM) binary classifiers (libSVM) with a fixed regulation parameter (C = 1) in order to compute a hyperplane that best separated the trial responses. Our use of a linear kernel is sensible under the assumption that it provides a plausible decoding mechanisms for downstream neurons [100,101].

Inputs for the pattern classifiers were extracted in two complementary approaches. The first approach used the pattern of voxel beta coefficients from the single-trial GLMs, which provided voxel patterns for each trial's Delay and Execute epochs. The second approach used the pattern of percent signal change values for each time point in the trial (i.e., time-resolved decoding) with respect to the time-course of a run-based averaged baseline value (-1, the imaging volume prior to the start of each trial), for all voxels in the ROI. Following the extraction of each trial's beta coefficients and/or time point voxel pattern, these values were standardized across voxels such that each voxel pattern had a mean of 0 and standard deviation of 1. Therefore, the mean univariate signal for each pattern was removed in the ROI. In order to derive main-effects of hand information (i.e., examine decoding of left hand vs. right hand movements) versus auditory cue information (examine decoding of "Compty" vs. "Midwig" cues) and increase statistical power, we performed separate analyses wherein we collapsed across auditory cue or hand, respectively. Our logic is that, when collapsing across auditory cue (i.e., re-labelling all trials based on the hand used), if we can observe decoding of hand information in auditory cortex during the Delay phase (prior to movement), then this information is represented with invariance to the cue, and thus sensory input.

For both decoding approaches, decoding accuracies for each subject were computed as the average classification accuracy across train-and-test iterations using a 'leave-one-run-out' cross-validation procedure. This procedure was performed separately for each ROI, trial epoch/timepoint (Delay and Execute in beta coefficient decoding, each timepoint in time-resolved decoding), and pairwise discrimination (left hand vs right hand movements, "Compty" vs "Midwig"). We statistically assessed decoding significance at the group-level using one-tailed t-tests vs. 50% chance decoding. To control for the problem of multiple comparisons within each ROI, we applied a Benjamini-Hochberg false-discovery rate (FDR) correction of $q<0.05$. Note that, for the time-resolved decoding approach, the data being used for classification at

any single time point (i.e., each TR) are independent, as they are full trial-lengths removed from directly adjacent trials (recall that each trial is, at minimum, equal to 24s), providing more than adequate time for the hemodynamic responses associated with individual TRs to sufficiently uncouple. Furthermore, the trial orders were fully randomized, and so any possible correlations between train and test data is not obvious and should not bias the data towards correct vs. incorrect classification [99,102].

Searchlight Pattern-Information Analyses

To complement our MVPA ROI analyses in the Experimental task, we also performed a pattern analysis in each subject using the searchlight approach [103]. Given the scope of this paper (i.e., to examine the top-down modulation of auditory cortex during planning), we constrained this searchlight analysis to (1) the auditory network mask defined by the Intact > Scrambled contrast using the independent auditory localizer data, and, (2) examine a main effect of hand information (i.e., decode left hand vs. right hand trials). In this procedure, the SVM classifier moved through each subjects' localizer-defined auditory network in a voxel-by-voxel fashion whereby, at each voxel, a sphere of surrounding voxels (radius of 4mm; 33 voxels) were extracted and input into the SVM classifier. The decoding accuracy for that sphere of voxels was then written to the central voxel. This searchlight procedure was performed separately with z-scored beta coefficient maps for the Delay and Execute epochs based on the GLM procedure described above, which yielded separate Delay and Execute decoding maps. To allow for group-level analyses, the decoding maps were smoothed (6mm FWHM Gaussian kernel) in each subject. Then, for each voxel, we assessed statistical significance using a one-tailed t-test versus 50% chance decoding. Group-level decoding maps for Delay and Execute epochs were thresholded at $p < .01$ and cluster corrected to $p < .05$ using Monte-Carlo style permutation tests with AFNI's 3dClustSim algorithm [104,105], which determined minimum cluster extents of 121 and 203 voxels for Delay and Execute epochs, respectively.

Behavioural Control Experiment

All subjects participated in a behavioural testing session (performed outside the MRI scanner and before the Experimental task) in which their eye fixations and forces corresponding to object grasping and lifting were measured as participants completed the Experimental task. This testing session was used for participant screening and to determine, from an analysis of their object lifting and eye-movement behaviour, whether participants were, respectively, (1) maintaining in working memory the instructed hand information over the delay period of each event-related trial and, (2) able to reliably maintain fixation over the duration of an fMRI experimental run (thereby arguing against classic alternative 'eye-movement confound' interpretations of the fMRI data). In this behavioural testing session, each participant completed 3 experimental runs, identical to those performed in the MRI scanner during the Experimental task testing session.

The experiment apparatus, equipment and setup was identical to that used in the MRI scanner, but testing was instead performed in the behavioural laboratory. Prior to beginning the behavioural experiment, participants received both verbal instructions and a demonstration by the experimenter as to how to correctly perform the object-directed actions. [Note that force measurements in this behavioural testing session were primarily taken only to provide additional confirmation that participants were capable of performing the task correctly.]

During this behavioural testing, an infrared video-based eye-tracking system (ETL 500 pupil/corneal tracking system, ISCAN Inc. Burlington, MA, USA), mounted below a headband, recorded the gaze position of the left eye at 240 Hz as the participant maintained gaze on the fixation LED. Gaze was calibrated using a two-step procedure: an initial 5-point calibration using ISCAN's Line-of-Sight Plane Intersection Software followed by a 25-point calibration routine. Twenty-five calibration points (4 mm-diameter circles) were shown on a cardboard frame, presented at the distance of the fixation point, and distributed over a region that incorporated the fixation point, the hand start

location, and the location of the central object position. The ISCAN calibration converted raw gaze signals into pixels from the line-of-sight camera and the 25-point calibration converted pixels (i.e., the output of the ISCAN calibration) into the coordinates of hand workspace. Gaze was calibrated at the start of the experimental run and was checked following each block of trials so that, if necessary, gaze could be re-calibrated before starting a new test block.

Acknowledgements

This work was supported by operating grants from the Canadian Institutes of Health Research (CIHR) awarded to J.R.F. and J.P.G. (MOP126158). J.P.G. was supported by a Natural Sciences and Engineering Research Council (NSERC) Discovery Grant, as well as funding from the Canadian Foundation for Innovation. D.J.G. was supported by a R.S. McLaughlin Fellowship and an NSERC graduate fellowship; C.N.A. was supported by an NSERC graduate fellowship. The authors would like to thank Adam McLean, Haitao Yang, Derek Quinlan, Martin York, Sean Hickman, and Don O'Brien for technical assistance.

Author Contributions

J.R.F., I.S.J and J.P.G. designed the experiment. D.J.G. and J.P.G. performed research. D.J.G., C.N.A., C.H., J.R.F and J.P.G., analyzed and interpreted data. D.J.G., J.R.F and J.P.G wrote the paper. All authors provided edits and feedback on the final version of the paper.

Competing Interests Statement

The authors declare no competing financial interests.

REFERENCES

1. Tanji, J. & Evarts, E. V. Anticipatory activity of motor cortex neurons in relation to direction of an intended movement. *J. Neurophysiol.* **39**, 1062–1068 (1976).
2. Messier, J. & Kalaska, J. F. Covariation of primate dorsal premotor cell activity with direction and amplitude during a memorized-delay reaching task. *J. Neurophysiol.* **84**, 152–165 (2000).
3. Riehle, A. & Requin, J. Monkey primary motor and premotor cortex: single-cell activity related to prior information about direction and extent of an intended movement. *J. Neurophysiol.* **61**, 534–549 (1989).
4. Churchland, M. M., Santhanam, G. & Shenoy, K. V. Preparatory activity in premotor and motor cortex reflects the speed of the upcoming reach. *J. Neurophysiol.* **96**, 3130–3146 (2006).
5. Shen, L. & Alexander, G. E. Preferential representation of instructed target location versus limb trajectory in dorsal premotor area. *J. Neurophysiol.* **77**, 1195–1212 (1997).
6. Pesaran, B., Nelson, M. J. & Andersen, R. A. Dorsal premotor neurons encode the relative position of the hand, eye, and goal during reach planning. *Neuron* **51**, 125–134 (2006).
7. Batista, A. P. *et al.* Reference Frames for Reach Planning in Macaque Dorsal Premotor Cortex. *Journal of Neurophysiology* **98**, 966–983 (2007).
8. Hocherman, S. & Wise, S. P. Effects of hand movement path on motor cortical activity in awake, behaving rhesus monkeys. *Exp. Brain Res.* **83**, 285–302 (1991).
9. Shenoy, K. V., Sahani, M. & Churchland, M. M. Cortical control of arm movements: a dynamical systems perspective. *Annu. Rev. Neurosci.* **36**, 337–359 (2013).
10. Elsayed, G. F., Lara, A. H., Kaufman, M. T., Churchland, M. M. & Cunningham, J. P. Reorganization between preparatory and movement population responses in motor cortex. *Nat. Commun.* **7**, 13239 (2016).
11. Churchland, M. M. *et al.* Neural population dynamics during reaching. *Nature* **487**, 51–56 (2012).
12. Churchland, M. M., Cunningham, J. P., Kaufman, M. T., Ryu, S. I. & Shenoy, K. V. Cortical preparatory activity: representation of movement or first cog in a dynamical machine? *Neuron* **68**, 387–400 (2010).
13. Ames, K. C., Ryu, S. I. & Shenoy, K. V. Neural dynamics of reaching following incorrect or absent motor preparation. *Neuron* **81**, 438–451 (2014).
14. Churchland, M. M. & Cunningham, J. P. A Dynamical Basis Set for Generating Reaches. *Cold Spring Harb. Symp. Quant. Biol.* **79**, 67–80 (2014).
15. Sussillo, D., Churchland, M. M., Kaufman, M. T. & Shenoy, K. V. A neural network that finds a naturalistic solution for the production of muscle activity. *Nat. Neurosci.* **18**, 1025–1033 (2015).
16. Russo, A. A. *et al.* Motor Cortex Embeds Muscle-like Commands in an Untangled Population Response. *Neuron* **97**, 953–966.e8 (2018).
17. Wolpert, D. M., Diedrichsen, J. & Flanagan, J. R. Principles of sensorimotor learning. *Nat. Rev. Neurosci.* **12**, 739–751 (2011).
18. Wolpert, D. M. & Flanagan, J. R. Motor prediction. *Current Biology* **11**, R729–R732 (2001).
19. Johansson & Flanagan, J. R. Coding and use of tactile signals from the fingertips in object

manipulation tasks. *Nat. Rev. Neurosci.* **10**, 345–359 (2009).
20. Flanagan, J. R., Bowman, M. C. & Johansson, R. S. Control strategies in object manipulation tasks. *Curr. Opin. Neurobiol.* **16**, 650–659 (2006).
21. Safstrom, D., Johansson, R. S. & Flanagan, J. R. Gaze behavior when learning to link sequential action phases in a manual task. *Journal of Vision* **14**, 3–3 (2014).
22. Schneider, D. M. & Mooney, R. How Movement Modulates Hearing. *Annual Review of Neuroscience* **41**, 553–572 (2018).
23. Crapse, T. B. & Sommer, M. A. Corollary discharge across the animal kingdom. *Nat. Rev. Neurosci.* **9**, 587–600 (2008).
24. Cisek, P., Crammond, D. J. & Kalaska, J. F. Neural activity in primary motor and dorsal premotor cortex in reaching tasks with the contralateral versus ipsilateral arm. *J. Neurophysiol.* **89**, 922–942 (2003).
25. Ames, K. C. & Churchland, M. M. Motor cortex signals corresponding to the two arms are shared across hemispheres, mixed among neurons, yet partitioned within the population response. doi:10.1101/552257
26. Nelson, A. *et al.* A circuit for motor cortical modulation of auditory cortical activity. *J. Neurosci.* **33**, 14342–14353 (2013).
27. Schneider, D. M., Nelson, A. & Mooney, R. A synaptic and circuit basis for corollary discharge in the auditory cortex. *Nature* **513**, 189–194 (2014).
28. Poulet, J. F. A. & Hedwig, B. A corollary discharge maintains auditory sensitivity during sound production. *Nature* **418**, 872–876 (2002).
29. Mandelblat-Cerf, Y., Las, L., Denisenko, N. & Fee, M. S. A role for descending auditory cortical projections in songbird vocal learning. *Elife* **3**, (2014).
30. Schneider, D. M., Nelson, A. & Mooney, R. A synaptic and circuit basis for corollary discharge in the auditory cortex. *Nature* **513**, 189–194 (2014).
31. Eliades, S. J. & Wang, X. Neural substrates of vocalization feedback monitoring in primate auditory cortex. *Nature* **453**, 1102–1106 (2008).
32. Reznik, D., Ossmy, O. & Mukamel, R. Enhanced auditory evoked activity to self-generated sounds is mediated by primary and supplementary motor cortices. *J. Neurosci.* **35**, 2173–2180 (2015).
33. Schneider, D. M., Sundararajan, J. & Mooney, R. A cortical filter that learns to suppress the acoustic consequences of movement. *Nature* **561**, 391–395 (2018).
34. Poeppel, D., Overath, T., Popper, A. N. & Fay, R. R. *The Human Auditory Cortex*. (Springer Science & Business Media, 2012).
35. Werner-Reiss, U., Kelly, K. A., Trause, A. S., Underhill, A. M. & Groh, J. M. Eye Position Affects Activity in Primary Auditory Cortex of Primates. *Current Biology* **13**, 554–562 (2003).
36. Reznik, D., Henkin, Y., Schadel, N. & Mukamel, R. Lateralized enhancement of auditory cortex activity and increased sensitivity to self-generated sounds. *Nat. Commun.* **5**, 4059 (2014).
37. Soon, C. S., Brass, M., Heinze, H.-J. & Haynes, J.-D. Unconscious determinants of free decisions in the human brain. *Nature Neuroscience* **11**, 543–545 (2008).
38. Harrison, S. A. & Tong, F. Decoding reveals the contents of visual working memory in early visual areas. *Nature* **458**, 632–635 (2009).
39. Gallivan, J. P., McLean, D. A., Valyear, K. F. & Culham, J. C. Decoding the neural mechanisms of human tool use. *Elife* **2**, e00425 (2013).
40. Lin, F.-H. *et al.* fMRI hemodynamics accurately reflects neuronal timing in the human brain measured by MEG. *NeuroImage* **78**, 372–384 (2013).
41. Gallivan, J. P., McLean, D. A., Flanagan, J. R. & Culham, J. C. Where one hand meets the

other: limb-specific and action-dependent movement plans decoded from preparatory signals in single human frontoparietal brain areas. *J. Neurosci.* **33**, 1991–2008 (2013).
42. Weinrich, M., Wise, S. P. & Mauritz, K. H. A neurophysiological study of the premotor cortex in the rhesus monkey. *Brain* **107 (Pt 2)**, 385–414 (1984).
43. Lara, Elsayed, G. F., Zimnik, A. J., Cunningham, J. P. & Churchland, M. M. Conservation of preparatory neural events in monkey motor cortex regardless of how movement is initiated. *Elife* **7**, (2018).
44. Kaufman, M. T. *et al.* Roles of monkey premotor neuron classes in movement preparation and execution. *J. Neurophysiol.* **104**, 799–810 (2010).
45. Pandarinath, C. *et al.* High performance communication by people with paralysis using an intracortical brain-computer interface. *Elife* **6**, (2017).
46. Wolpert, D. M. & Flanagan, J. R. Motor prediction. *Curr. Biol.* **11**, R729–32 (2001).
47. Johansson & Flanagan, J. R. Coding and use of tactile signals from the fingertips in object manipulation tasks. *Nat. Rev. Neurosci.* **10**, 345–359 (2009).
48. Flanagan, J. R., Bowman, M. C. & Johansson, R. S. Control strategies in object manipulation tasks. *Curr. Opin. Neurobiol.* **16**, 650–659 (2006).
49. Shergill, S. S., Bays, P. M., Frith, C. D. & Wolpert, D. M. Two eyes for an eye: the neuroscience of force escalation. *Science* **301**, 187 (2003).
50. Bays, P. M., Wolpert, D. M. & Flanagan, J. R. Perception of the consequences of self-action is temporally tuned and event driven. *Curr. Biol.* **15**, 1125–1128 (2005).
51. Bays, P. M., Flanagan, J. R. & Wolpert, D. M. Attenuation of self-generated tactile sensations is predictive, not postdictive. *PLoS Biol.* **4**, e28 (2006).
52. Holst, E. von, von Holst, E. & Mittelstaedt, H. Das Reafferenzprinzip. *Naturwissenschaften* **37**, 464–476 (1950).
53. Scott, S. H. The computational and neural basis of voluntary motor control and planning. *Trends Cogn. Sci.* **16**, 541–549 (2012).
54. Scott, S. H. A Functional Taxonomy of Bottom-Up Sensory Feedback Processing for Motor Actions. *Trends Neurosci.* **39**, 512–526 (2016).
55. Jenmalm, P., Schmitz, C., Forssberg, H. & Ehrsson, H. H. Lighter or heavier than predicted: neural correlates of corrective mechanisms during erroneously programmed lifts. *J. Neurosci.* **26**, 9015–9021 (2006).
56. Desmurget, M. *et al.* Role of the posterior parietal cortex in updating reaching movements to a visual target. *Nat. Neurosci.* **2**, 563–567 (1999).
57. Tunik, E., Frey, S. H. & Grafton, S. T. Virtual lesions of the anterior intraparietal area disrupt goal-dependent on-line adjustments of grasp. *Nat. Neurosci.* **8**, 505–511 (2005).
58. Otazu, G. H., Tai, L.-H., Yang, Y. & Zador, A. M. Engaging in an auditory task suppresses responses in auditory cortex. *Nat. Neurosci.* **12**, 646–654 (2009).
59. Schneider, D. M., Nelson, A. & Mooney, R. A synaptic and circuit basis for corollary discharge in the auditory cortex. *Nature* **513**, 189–194 (2014).
60. Foxe, J. J. *et al.* Auditory-somatosensory multisensory processing in auditory association cortex: an fMRI study. *J. Neurophysiol.* **88**, 540–543 (2002).
61. Schürmann, M., Caetano, G., Hlushchuk, Y., Jousmäki, V. & Hari, R. Touch activates human auditory cortex. *Neuroimage* **30**, 1325–1331 (2006).
62. Lakatos, P., Chen, C.-M., O'Connell, M. N., Mills, A. & Schroeder, C. E. Neuronal oscillations and multisensory interaction in primary auditory cortex. *Neuron* **53**, 279–292 (2007).
63. Kayser, C., Petkov, C. I., Augath, M. & Logothetis, N. K. Integration of touch and sound in auditory cortex. *Neuron* **48**, 373–384 (2005).

64. Johansson & Flanagan, J. R. Coding and use of tactile signals from the fingertips in object manipulation tasks. *Nat. Rev. Neurosci.* **10**, 345–359 (2009).
65. Reep, R. L., Corwin, J. V., Hashimoto, A. & Watson, R. T. Afferent connections of medial precentral cortex in the rat. *Neurosci. Lett.* **44**, 247–252 (1984).
66. Reep, R. L., Corwin, J. V., Hashimoto, A. & Watson, R. T. Efferent connections of the rostral portion of medial agranular cortex in rats. *Brain Res. Bull.* **19**, 203–221 (1987).
67. Nelson, A. *et al.* A Circuit for Motor Cortical Modulation of Auditory Cortical Activity. *Journal of Neuroscience* **33**, 14342–14353 (2013).
68. Deacon, T. W. Cortical connections of the inferior arcuate sulcus cortex in the macaque brain. *Brain Res.* **573**, 8–26 (1992).
69. Petrides, M. & Pandya, D. N. Association fiber pathways to the frontal cortex from the superior temporal region in the rhesus monkey. *J. Comp. Neurol.* **273**, 52–66 (1988).
70. Petrides, M. & Pandya, D. N. Comparative cytoarchitectonic analysis of the human and the macaque ventrolateral prefrontal cortex and corticocortical connection patterns in the monkey. *Eur. J. Neurosci.* **16**, 291–310 (2002).
71. Romanski, L. M. *et al.* Dual streams of auditory afferents target multiple domains in the primate prefrontal cortex. *Nat. Neurosci.* **2**, 1131–1136 (1999).
72. Propper, R. E. *et al.* A combined fMRI and DTI examination of functional language lateralization and arcuate fasciculus structure: Effects of degree versus direction of hand preference. *Brain and Cognition* **73**, 85–92 (2010).
73. Powell, H. W. R. *et al.* Hemispheric asymmetries in language-related pathways: a combined functional MRI and tractography study. *Neuroimage* **32**, 388–399 (2006).
74. Serrien, D. J., Ivry, R. B. & Swinnen, S. P. Dynamics of hemispheric specialization and integration in the context of motor control. *Nat. Rev. Neurosci.* **7**, 160–166 (2006).
75. Serrien, D. J. & Spapé, M. M. The role of hand dominance and sensorimotor congruence in voluntary movement. *Exp. Brain Res.* **199**, 195–200 (2009).
76. Haaland, K. Y., Elsinger, C. L., Mayer, A. R., Durgerian, S. & Rao, S. M. Motor sequence complexity and performing hand produce differential patterns of hemispheric lateralization. *J. Cogn. Neurosci.* **16**, 621–636 (2004).
77. Friederici, A. D. Pathways to language: fiber tracts in the human brain. *Trends Cogn. Sci.* **13**, 175–181 (2009).
78. Gallivan, J. P., Chapman, C. S., Gale, D. J., Flanagan, J. R. & Culham, J. C. Selective Modulation of Early Visual Cortical Activity by Movement Intention. *Cereb. Cortex* (2019). doi:10.1093/cercor/bhy345
79. Gutteling, T. P. *et al.* Action preparation shapes processing in early visual cortex. *J. Neurosci.* **35**, 6472–6480 (2015).
80. Chapman, C. S., Gallivan, J. P., Culham, J. C. & Goodale, M. A. Mental blocks: fMRI reveals top-down modulation of early visual cortex when obstacles interfere with grasp planning. *Neuropsychologia* **49**, 1703–1717 (2011).
81. Steinmetz, N. A. & Moore, T. Eye Movement Preparation Modulates Neuronal Responses in Area V4 When Dissociated from Attentional Demands. *Neuron* **83**, 496–506 (2014).
82. Matyas, F. *et al.* Motor control by sensory cortex. *Science* **330**, 1240–1243 (2010).
83. Scheich, H., Brechmann, A., Brosch, M., Budinger, E. & Ohl, F. W. The cognitive auditory cortex: task-specificity of stimulus representations. *Hear. Res.* **229**, 213–224 (2007).
84. Weinberger, N. M. Reconceptualizing the Primary Auditory Cortex: Learning, Memory and Specific Plasticity. *The Auditory Cortex* 465–491 (2011). doi:10.1007/978-1-4419-0074-6_22
85. Huang, Y., Heil, P. & Brosch, M. Associations between sounds and actions in early auditory

cortex of nonhuman primates. *Elife* **8**, (2019).
86. Oldfield, R. C. The assessment and analysis of handedness: the Edinburgh inventory. *Neuropsychologia* **9**, 97–113 (1971).
87. Gallivan, J. P., Johnsrude, I. S. & Flanagan, J. R. Planning Ahead: Object-Directed Sequential Actions Decoded from Human Frontoparietal and Occipitotemporal Networks. *Cereb. Cortex* **26**, 708–730 (2016).
88. Gallivan, J. P., Cant, J. S., Goodale, M. A. & Flanagan, J. R. Representation of object weight in human ventral visual cortex. *Curr. Biol.* **24**, 1866–1873 (2014).
89. Jenkinson, M., Beckmann, C. F., Behrens, T. E. J., Woolrich, M. W. & Smith, S. M. FSL. *NeuroImage* **62**, 782–790 (2012).
90. Friston, K. J. *Statistical Parametric Mapping: The Analysis of Functional Brain Images*. (Elsevier, 2007).
91. Gorgolewski, K. *et al.* Nipype: a flexible, lightweight and extensible neuroimaging data processing framework in python. *Front. Neuroinform.* **5**, 13 (2011).
92. Mumford, J. A., Turner, B. O., Ashby, F. G. & Poldrack, R. A. Deconvolving BOLD activation in event-related designs for multivoxel pattern classification analyses. *Neuroimage* **59**, 2636–2643 (2012).
93. Morosan, P. *et al.* Population maps of cytoarchitectonically defined human auditory areas. *NeuroImage* **11**, S304 (2000).
94. Da Costa, S. *et al.* Human primary auditory cortex follows the shape of Heschl's gyrus. *J. Neurosci.* **31**, 14067–14075 (2011).
95. Morosan, P. *et al.* Human primary auditory cortex: cytoarchitectonic subdivisions and mapping into a spatial reference system. *Neuroimage* **13**, 684–701 (2001).
96. Rademacher, J. *et al.* Probabilistic mapping and volume measurement of human primary auditory cortex. *Neuroimage* **13**, 669–683 (2001).
97. Desikan, R. S. *et al.* An automated labeling system for subdividing the human cerebral cortex on MRI scans into gyral based regions of interest. *Neuroimage* **31**, 968–980 (2006).
98. Hackett, T. A. *et al.* Feedforward and feedback projections of caudal belt and parabelt areas of auditory cortex: refining the hierarchical model. *Front. Neurosci.* **8**, 72 (2014).
99. Abraham, A. *et al.* Machine learning for neuroimaging with scikit-learn. *Front. Neuroinform.* **8**, 14 (2014).
100. Shamir, M. & Sompolinsky, H. Implications of neuronal diversity on population coding. *Neural Comput.* **18**, 1951–1986 (2006).
101. DiCarlo, J. J. & Cox, D. D. Untangling invariant object recognition. *Trends Cogn. Sci.* **11**, 333–341 (2007).
102. Misaki, M., Kim, Y., Bandettini, P. A. & Kriegeskorte, N. Comparison of multivariate classifiers and response normalizations for pattern-information fMRI. *Neuroimage* **53**, 103–118 (2010).
103. Kriegeskorte, N., Goebel, R. & Bandettini, P. Information-based functional brain mapping. *Proc. Natl. Acad. Sci. U. S. A.* **103**, 3863–3868 (2006).
104. Cox, R. W. AFNI: software for analysis and visualization of functional magnetic resonance neuroimages. *Comput. Biomed. Res.* **29**, 162–173 (1996).
105. Cox, R. W., Chen, G., Glen, D. R., Reynolds, R. C. & Taylor, P. A. FMRI Clustering in AFNI: False-Positive Rates Redux. *Brain Connect.* **7**, 152–171 (2017).